First-principles calculations of the electronic and phonon properties of APt_{3}P (A = Ca, Sr, and La): Evidence for a charge-density-wave instability and a soft phonon

Hui Chen, Xiaofeng Xu, Chao Cao, and Jianhui Dai

Phys. Rev. B **86**, 125116 — Published 13 September 2012

DOI: 10.1103/PhysRevB.86.125116

Charge Density Wave Instability and Soft Phonon in APt$_3$P (A=Ca, Sr, and La)

Hui Chen, Xiaofeng Xu, Chao Cao,* and Jianhui Dai†
Condensed Matter Physics Group, Department of Physics, Hangzhou Normal University, Hangzhou 310036, China
(Dated: Jul. 16, 2012)

The electronic and phonon properties of the platinum pnictide superconductors APt$_3$P (A=Ca, Sr, and La) were studied using first-principles calculations. The spin-orbit coupling effect is significant in LaPt$_3$P but negligible in CaPt$_3$P and SrPt$_3$P. Moreover, SrPt$_3$P has been demonstrated to exhibit an unexpected weak charge-density-wave (CDW) instability which is neither simply related to the Fermi-surface nesting nor to the momentum-dependent electron-phonon coupling alone. The instability is absent in CaPt$_3$P and can be quickly suppressed by the external pressure, accompanied with decreases in the phonon softening and BCS T_c. Our results suggest SrPt$_3$P as a rare example where superconductivity is enhanced by the CDW fluctuations.

PACS numbers: 74.20.Pq, 71.45.Lr, 74.70.Dd

I. INTRODUCTION

The discovery of iron-based high-Tc superconductors has stimulated considerable interests in the condensed matter physics society. Sharing the similar layered square lattice crystal structures, both iron-pnictides/chalcogenides and cuprates exhibit the long-range magnetic order in parent compounds and the unconventional superconductivity (SC) upon doping[1–6]. In these 3d transition-metal based materials, the electron correlation effect is considered to play a role in the formation of the spin-density-wave (SDW) instability while the electron pairing may be mediated or enhanced by the spin fluctuations.

Recently, several families of platinum-pnictide based superconductors(SrPtAs[7], SrPt$_2$As$_2$[8], APt$_3$P[9]) have been reported. Among these compounds, APt$_3$P (A=Ca, Sr, and La) have shown considerable peculiarity. The crystal structures of these 5d electron-based pnictides are experimentally determined to be anti-pevroskite with $\sqrt{2}\times\sqrt{2}\times 1$ distortion (FIG. 1). Due to the distortion, the platinum atoms take two different sites Pt$^{\rm I}$ and Pt$^{\rm II}$, while the Pt$^{\rm II}$ and P atoms form a Pt$_2$P layer that resembles the iron-pnictide layers in the iron-based superconductors(FIG. 1(b)). A particularly interesting feature of this family is the significant variation of T_c, i.e., T_c = 1.5K, 6.6K, and 8.4K for A =La, Ca, and Sr, respectively. Among them, SrPt$_3$P seems to be very special, as it has not only the highest T_c in the 5d-electron based superconductors, but also a large $2\Delta_0/k_BT_c\sim 5$, manifesting strong-coupling BCS superconductivity. It also exhibits a substantially lower electron specific heat coefficient γ than its homologue CaPt$_3$P and a notable anomaly near 10K slightly above T_c.

There are two major distinctions between the 3d and 5d transition metal pnictides. First, the 5d-orbitals are usually more extended so that the Coulomb interaction is relatively weak. Second, the spin-orbit coupling (SOC) in 5d-electrons is much stronger, as exemplified by the chemically similar compound SrPtAs[7]. In order to understand the puzzling features observed in the ASr$_3$P family, it is necessary and informative to clarify the spin-orbit coupling (SOC) and the electron-phonon coupling effects in the electronic structure of these materials.

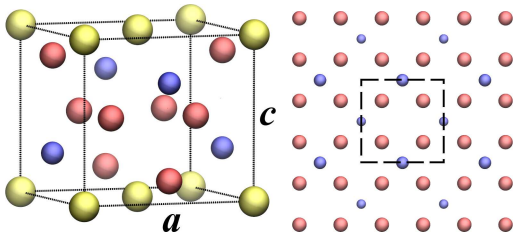

(a)Crystal Structure (b)Pt$_2$P layer

FIG. 1: (color online) Crystal structure of APt$_3$P compounds. (a) Crystal structure of APt$_3$P. Yellow atoms are A (Ca, Sr, or La) atoms; red atoms are platinum; and blue atoms are phosphorus. (b) Pt$^{\rm II}$ and P atoms form a Pt$_2$P layer that is geometrically similar to the iron-arsenic layer in the iron-pnictides. Larger blue atoms denote the P atoms above the Pt plane and smaller blue atoms are the ones below the Pt plane.

In this article, we present our latest first principles results of APt$_3$P (A=Ca, Sr, and La). We show that while spin-orbit coupling effect is negligible in SrPt$_3$P and CaPt$_3$P, it significantly affects the electronic structure of LaPt$_3$P around the Fermi level E_F. An unexpected weak charge-density-wave (CDW) instability develops in the SrPt$_3$P which is neither simply related to the Fermi-surface nesting nor to the momentum-dependent electron-phonon coupling alone. The instability is absent in CaPt$_3$P and can be quickly suppressed by the external pressure, accompanied with decreases in the BCS T_c. The CDW also reduces the electron density of states (DOS) around E_F for SrPt$_3$P, leading to the anomalous specific heat behavior around 10K.

The rest of this paper is organized as follows. In the next section, we briefly introduces the calculation method and details, followed by a section where we present in detail the electronic structure of APt$_3$P (A=Sr, Ca, and La), the phonon properties of SrPt$_3$P compared with

	$SrPt_3P$	$CaPt_3P$	$LaPt_3P$
a (Å)	5.8788 (5.8852)	5.7264 (5.7284)	5.8187 (5.8221)
c (Å)	5.4313 (5.4339)	5.4507 (5.4618)	5.5230 (5.5273)
$z^{\rm I}_{\rm Pt}$	0.1376 (0.1394)	0.1370 (0.1382)	0.1435 (0.1443)
$z_{\rm P}$	0.2767 (0.2754)	0.2686 (0.2672)	0.2717 (0.2707)

TABLE I: Optimized geometry of APt_3P. $z^{\rm I}_{\rm Pt}$ denotes the fractional z-coordinate of $Pt^{\rm I}$ site. The numbers outside (inside) the brackets are obtained without (with) SOC.

$CaPt_3P$, as well as electron-phonon interactions and theoretical T_c of $SrPt_3P$. We finally summarize and draw conclusions in section III.

II. METHOD AND CALCULATION DETAILS

To study the electronic structure of APt_3P, we employed the plane -wave basis projected augmented wave density functional (DFT) method implemented in the Vienna ab-initio simulation package (VASP)[10,11]. The phonon properties were obtained using the frozen phonon method implemented in PHONOPY[12]. To ensure the calculation convergency to 1meV/cell, a 480 eV energy cutoff to the plane-wave basis and a $8\times8\times8$ Monkhorst-Pack **k**-grid were employed to perform structural relaxation until the maximum force on individual atoms is smaller than 0.001 eV/Å and the internal stress smaller than 0.01 kbar. The DOS results are obtained using $16\times16\times16$ Γ-centered **k**-grid and the tetrahedra method. For electron-phonon coupling calculations and superconducting T_c estimation, we used density functional perturbation theory implemented in the *Quantum Espresso* package[13], where the electron-phonon coupling constants were evaluated with $4\times4\times4$ Γ-centered phonon **q**-grid and $32\times32\times32$ Γ- centered **k**-mesh.

III. RESULTS AND DISCUSSION

A. Geometry and Electronic Structures

The optimized structural parameters are summarized in TABLE I, which agree very well with the experimental results[9] (<3% difference). Thus the application of the DFT(+SOC) method is guaranteed in these materials with a relatively weak Coulomb interaction. We then explore the electronic structures shown in FIG. 2. For both $SrPt_3P$ and $CaPt_3P$, the SOC does not affect the electronic structure around the Fermi energy E_F, as no band splitting due to the SOC is observed within $\sim E_F\pm500$ meV range. Hence the Fermi surfaces and consequently the SC of these two compounds are not affected by the SOC effect. The situation is, however, quite different in the case of $LaPt_3P$, as it exhibits a significant band splitting due to the SOC effect from M to X around E_F, where an extra Fermi surface sheet emerges. This observation accounts for the significant reduction of T_c in $LaPt_3P$ because the SOC-induced band splitting breaks the spin symmetry and thus reduces the pairing strength of the electrons. Consequently, $LaPt_3P$ may be a new member of the unconventional superconductors like SrPtAs[14] which deserves further experimental study. In the rest of our discussions, we will mainly focus on $SrPt_3P$ and $CaPt_3P$.

Similarities between their electronic structures are expected, since both Sr and Ca are iso-valent alkaline earth elements with two outmost s-electrons. Projected density of states (PDOS) plots (FIG. 2(d)-(e)) suggest that the DOS around E_F in both compounds are dominated by Pt-5d and P-2p orbitals, while the contribution from Sr or Ca orbitals are minimum. However, the band structures of $SrPt_3P$ and $CaPt_3P$ show two significant differences around E_F. First, one of the hole bands crossing E_F around the Z point in $SrPt_3P$ is missing in $CaPt_3P$. Thus $CaPt_3P$ has one less Fermi surface sheets than $SrPt_3P$(FIG. 3). Second, two bands cross E_F at approximately the same **k** point in $SrPt_3P$ from Γ to M, while these crossing **k** points are well separated in $CaPt_3P$.

B. Phonon Properties and Charge-Density-Wave Instability

We further investigate the mechanical properties of these materials by performing phonon calculations using the frozen phonon method. For $SrPt_3P$, the resulting phonon band structure and DOS exhibit a clear instability evidenced by the appearance of the imaginary phonon frequencies. Remarkably, such instability is absent in $CaPt_3P$. Usually, two scenarios can be responsible for this instability, namely, the SDW and CDW, respectively. The former appears frequently in the 3d-transition-metal pnictide superconductors. We performed calculations with four possible spin configurations including/excluding the SOC. All these calculations eventually converge to the non-magnetic spin configuration. Thus we exclude the SDW instability in this system.

Noting that the soft phonon modes are located around the X (π, π, 0) and R (π, π, π) points (FIG. 5(a)), we then used a $\sqrt{2}\times\sqrt{2}\times1$ supercell with respect to its original unit cell to adapt the lattice distortions due to the possible CDW instability. A less than 0.2% distortion to the atomic coordinates with $\sqrt{2}\times\sqrt{2}\times1$ modulation is found to lower the total energy by ~ 10 meV/cell (or ~ 5 meV/formula). It is also confirmed that the soft phonon mode disappears if the distorted supercell is used as the static initial condition to calculate phonon properties. Therefore, we demonstrated that the soft phonon modes are in fact due to the CDW instability in $SrPt_3P$. It is important to emphasize that the energy scale of the predicted CDW instability is about ~ 1 meV/atom, which is at least one order smaller than the SDW energy scale in iron pnictides. This indicates the CDW temperature

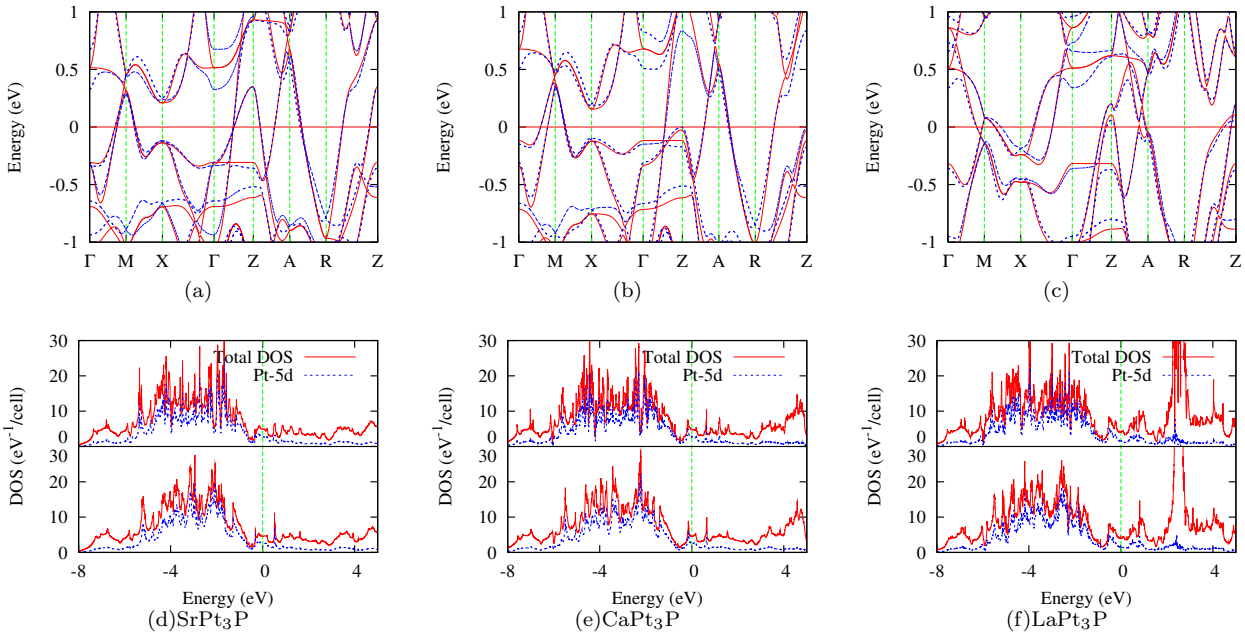

FIG. 2: Band structure and DOS of (a)(d) $SrPt_3P$, (b)(e) $CaPt_3P$, and (c)(f) $LaPt_3P$ at ambient pressure (0 GPa) with and without SOC. (a)-(c) are band structures, where red solid lines and blue dashed lines are obtained without and with SOC, respectively. (d)-(f) show DOS and its projection onto Pt-5d orbitals, with upper panels and lower panels showing the results with and without SOC, respectively.

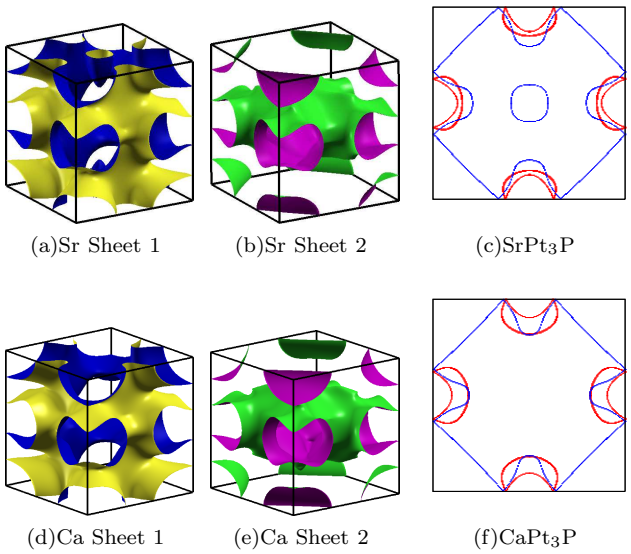

FIG. 3: (color online)Fermi surface sheets of (a-b) $SrPt_3P$ and (d-e) $CaPt_3P$ at 0 GPa. Fermi surface cross section of (e) $SrPt_3P$ and (f) $CaPt_3P$ at $k_z = 0.0$ (red) and $k_z = 0.5$ (blue). The centers of the squares are Γ(Z) and the corners are X. Notice that $CaPt_3P$ has one less fermi surface sheet around Z.

is roughly around 10 K or even lower in $SrPt_3P$. Further calculations show that the weak CDW instability is greatly suppressed by applying an external pressure and

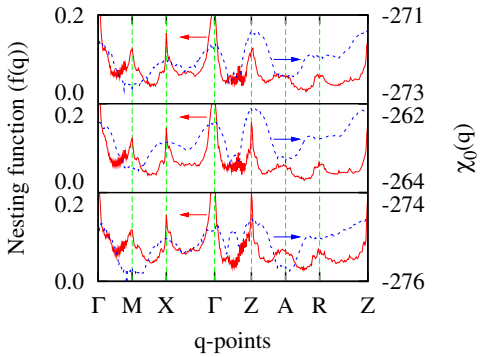

FIG. 4: (color online) Fermi surface nesting function ($f(\mathbf{q})$, red solid lines) and electron response function ($\chi_0(\mathbf{q})$, blue dashed lines) for $SrPt_3P$ at 0GPa (top panel) and 5GPa (middle panel), as well as $CaPt_3P$ at 0GPa (bottom panel).

disappears above 3 GPa.

We next investigate the correlation between the CDW instability and the crystal structure by showing the evolution of the phonon DOS of $SrPt_3P$ under the external pressure(FIG. 5). At zero GPa, a DOS hump below 0 THz is clearly presented due to the soft phonon modes caused by the CDW instability as shown above. The first real phonon DOS peak is formed around 2 THz, primarily contributed by the lowest optical modes. The external pressure compresses the interatomic distance, causing stiffer bonds, and therefore all real phonon modes shift to higher energies. For the soft modes, the DOS hump below

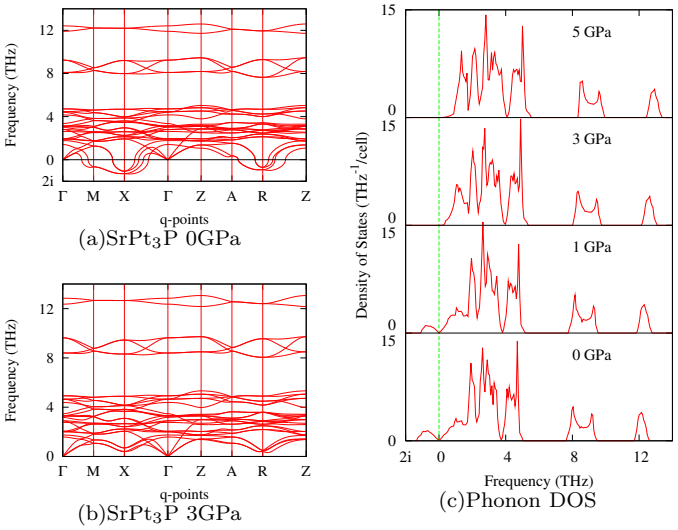

FIG. 5: (a)-(b): Phonon band structure of $SrPt_3P$ at (a) 0 GPa and (b) 3 GPa. (c): Phonon density of states under different pressures. Negative frequencies indicate the imaginary (soft) phonon modes caused by CDW instability.

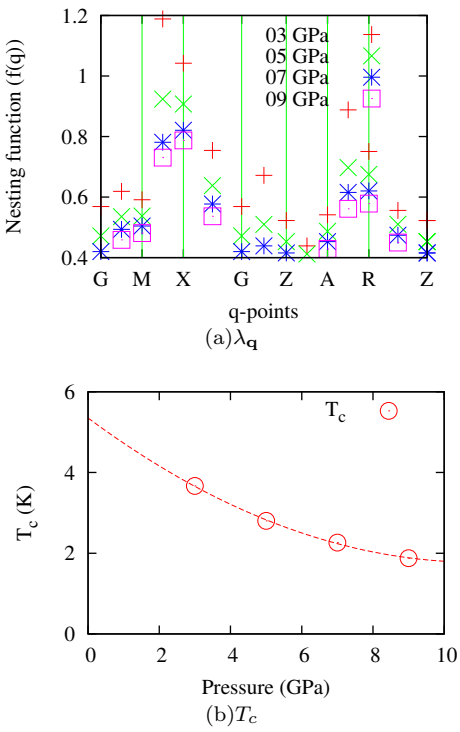

FIG. 6: (a) **q**-dependent electron-phonon coupling constant $\lambda_{\mathbf{q}}$ of $SrPt_3P$ under different pressures. (b)SC transition temperature T_c of $SrPt_3P$ at different pressures. The circles in (b) indicates the T_c obtained by first-principles electron-phonon coupling calculations and the Allen-Dynes formula; and the dashed line is a quadratic curve fitted to the results.

0 THz is reduced at 1 GPa and eventually disappears at 3 GPa, indicating that the CDW instability can be quickly suppressed by the external pressure. The *hardened* soft modes contribute to the states below 2 THz, forming the new first peak below 2 THz.

To analyze the formation of the CDW instability, we calculated the Fermi surface nesting function $f(\mathbf{q}) = \frac{2}{N_{\mathbf{k}}}\sum_{\mathbf{k}mn}\delta(\epsilon_{\mathbf{k}+\mathbf{q}n})\delta(\epsilon_{\mathbf{k}m})$ and the non-interacting electron response function $\chi_0(\mathbf{q}) = \frac{1}{N_{\mathbf{k}}}\sum_{\mathbf{k}mn}\frac{f_{\mathbf{k}+\mathbf{q}n}-f_{\mathbf{k}m}}{\epsilon_{\mathbf{k}+\mathbf{q}n}-\epsilon_{\mathbf{k}m}}$ for $SrPt_3P$ at different pressures, as well as for $CaPt_3P$ at 0 GPa (FIG. 4)[26]. In all these cases, no significant divergence appears in both functions. Instead, $f(\mathbf{q})$ shows peaks not only around X, but also around M, and Z. In the cases of $SrPt_3P$ at 5 GPa and $CaPt_3P$ at 0 GPa, the nesting functions show even stronger peaks around Z. Besides, $\chi_0(\mathbf{q})$ shows broad humps instead of sharp peaks around X, and that feature does not show much variation. Thus the Fermi surface nesting effect alone cannot be responsible for the CDW instability. Recently, it was suggested that in the dichalcogenides the CDW could be a result of strong electron-phonon coupling at certain $\mathbf{q}$ vectors[15–17]. If this is the case here, the $\mathbf{q}$-resolved electron-phonon coupling constant $\lambda_{\mathbf{q}}$ of $SrPt_3P$ should exhibit an apparent anomaly around the CDW wave vector at 0 GPa, which would then be suppressed by external pressure and disappear beyond 3 GPa. In order to clarify this possibility, we performed first-principles electron-phonon calculation at different pressures (FIG. 6(a)). The resulting wave vector, however, is around ($\pi/2$, π, 0), far from the predicted CDW vector (π, π, 0). Therefore, the electron-phonon coupling alone cannot be accounted for the present CDW instability either.

C. Superconducting T_c and Specific Heat Anomaly

We now discuss the T_c of $SrPt_3P$ within the BCS theory. A direct calculation of T_c is prohibited due to the presence of the CDW-induced imaginary phonon modes. We thus performed a series of calculations at the pressures from 3 to 9 GPa, where the CDW instability is absent. The variation of the BCS T_c under the external pressure p is obtained by using the Allen-Dynes formula[18], and then extrapolated to $p = 0$ with least square fitting method assuming a quadratic dependence of T_c on p(FIG. 6(b)). Hence the extrapolation represents the T_c without the CDW instability. The resulting transition temperature is 5.4 K, much lower than the 8.4 K as observed in experiment. The large difference between the calculated and experimental T_c may be an evidence for CDW-enhanced superconductivity.

In addition to T_c, the experiment reveals that the specific heat coefficient γ, which is proportional to the electron DOS at the Fermi level $g(E_F)$, is relatively larger in $CaPt_3P$. Our calculation shows that in the absence of the CDW, $g(E_F)$ is 4.58 eV^{-1}/cell for $SrPt_3P$, which is slightly larger than the corresponding value 4.53 eV^{-1}/cell for $CaPt_3P$. We then performed the DOS calculations using a $\sqrt{2} \times \sqrt{2} \times 1$ super cell that accom-

modates CDW distortions. The resulting $g(E_F) = 4.31$ eV^{-1}/cell, which is 6% smaller than the one without CDW. Thus the formation of the CDW indeed leads to a sizable reduction in γ, in agreement with the experiment. The experimental data also reveal other delicacies related to the specific heat and resistivity in $SrPt_3P$ slightly above the T_c. While these features remain questionable, we note that these features are just within the energy scale $\sim$ 10K where the CDW instability starts to play a role.

Several remarks are then in order. First, the CDW instability predicted for $SrPt_3P$ is rather unexpected. This is because of not only the relatively high $T_c \sim 8.4$K observed in the 5*d* transition metal compounds, but also the very small CDW energy scale $T^* \sim 10$K compared to the canonical CDW superconductors such as in a series of transition metal dichalcogenides $TiSe_2$[19–21] and $NbSe_2$[22,23], as well as another platinum pnictide compound $SrPt_2As_2$[8]. So far the minimal difference between the CDW and SC temperatures in known CDW materials is observed in $NbSe_2$ with $T_c = 7.2$K and $T^* = 32$K. Second, while the CDW order competes and sometimes co-exists with the SC in most of known CDW superconductors, the CDW in these cases is *static*, in the sense that the charge redistribution and ionic modulation are already stabilized and occur far above the SC instability. In the present case, however, the CDW instability should be considered as *dynamical*, because only a very small distortion (less than 0.2%) in atomic coordinates is required to avoid the imaginary phonon modes and accommodate the lattice modulation, resulting in a very small characteristic temperature ($\sim$ 10K). Perhaps this is the reason why the CDW in $SrPt_3P$ has not been reported so far experimentally. It is also possible that quantum fluctuations may influence the weak CDW, resulting in quantum paraelectric states, similar to the ferroelectric state of $SrTiO_3$. Third, in contrast to the conventional mechanism of the CDW, neither pure nesting effect nor the momentum-dependence of the electron-phonon coupling can account to the CDW formation in $SrPt_3P$ independently. This implies that an appropriate combination of the nestings, their frustrations, the electron-phonon coupling, or even the states far away from the Fermi-surface, is at work in stabilizing the CDW in realistic materials[24]. We argue that this may be a characteristic feature of the dynamical CDW.

IV. CONCLUSION

In conclusion, we have performed a detailed study on APt_3P using the first-principles simulations. Our calculations show that the Fermi surfaces of these materials consist of multiple sheets. The spin-orbit coupling effect is negligible in both $SrPt_3P$ and $CaPt_3P$ but plays an important role in $LaPt_3P$. We predict that $SrPt_3P$ exhibits a CDW instability which can be quickly suppressed by the external pressure and is absent in $CaPt_3P$ under ambient pressure. The formation of the CDW is neither directly related to the nesting effect nor to the electron-phonon coupling alone. Our results suggest that $SrPt_3P$ is a rare material where the SC instability falls into the fluctuation regime of the dynamical CDW which in turn leads to the enhancement in T_c.

Acknowledgement. The authors would like to thank B. Chen, X.-Y. Feng and N.L. Wang for valuable discussions. This work was supported in part by the NSF of China (No. 11274006, 11274084, and 11104051), the 973 Project of the MOST, and the NSF of Zhejiang Province (No. LR12A04003 and Z6110033). All the calculations were performed at the high performance computing center of Hangzhou Normal University.

Note added. During the preparation of this manuscript, we became aware of another work by I. A. Nekrasov and M. V. Sadovskii[25] on the electronic structure of $SrPt_3P$. However, they did not consider the spin-orbit coupling effect, the phonon properties, nor the possible CDW instability in this material.

* E-mail address: ccao@hznu.edu.cn
† E-mail address: daijh@hznu.edu.cn

[1] C. de la Cruz, Q. Huang, J. W. Lynn, J. Li, W. R. II, J. L. Zarestky, H. A. Mook, G. F. Chen, J. L. Luo, N. L. Wang, et al., Nature **453** (2008).
[2] J. Dong, et al., Europhys. Lett. **83**, 27006 (2008).
[3] Q. Huang, Y. Qiu, W. Bao, M. A. Green, J. W. Lynn, Y. C. Gasparovic, T. Wu, G. Wu, and X. H. Chen, Phys. Rev. Lett. **101**, 257003 (2008).
[4] W. Bao, Y. Qiu, Q. Huang, M. A. Green, P. Zajdel, M. R. Fitzsimmons, M. Zhernenkov, S. Chang, M. Fang, B. Qian, et al., Phys. Rev. Lett. **102**, 247001 (2009).
[5] F. Ma, W. Ji, J. Hu, Z.-Y. Lu, and T. Xiang, Phys. Rev. Lett. **102**, 177003 (2009).
[6] W. Bao, Q. Huang, G. F. Chen, M. A. Green, D. M. Wang, J. B. He, X. Q. Wang, and Y. Qiu, Chin. Phys. Lett. **28** (2011).
[7] Y. Nishikubo, K. Kudo, and M. Nohara, J. Phys. Soc. Jap. **80**, 055002 (2011).
[8] K. Kudo, Y. Nishikubo, and M. Nohara, J. Phys. Soc. Jap. **79**, 123710 (2010).
[9] T. Takayama, K. Kuwano, D. Hirai, Y. Katsura, A. Yamamoto, and H. Takagi, Phys. Rev. Lett. **108**, 237001 (2012).
[10] G. Kresse and J. Hafner, Phys. Rev. B **47**, 558 (1993).
[11] G. Kresse and D. Joubert, Phys. Rev. B **59**, 1758 (1999).
[12] A. Togo, F. Oba, and I. Tanaka, Phys. Rev. B **78**, 134106 (2008).
[13] P. Giannozzi, S. Baroni, N. Bonini, and M. Calandra, et al., J. Phys. Cond. Mat. **21**, 395502 (2009).
[14] S. J. Youn, M. H. Fischer, S. H. Rhim, M. Sigrist, and D. Agterberg, arXiv:1111.5058 (2011).
[15] F. Weber, S. Rosenkranz, J.-P. Castellan, R. Osborn, R. Hott, R. Heid, K.-P. Bohnen, T. Egami, A. H. Said, and D. Reznik, Phys. Rev. Lett. **107**, 107403 (2011).
[16] M. Calandra and F. Mauri, Phys. Rev. Lett. **106**, 196406 (2011).
[17] M. D. Johannes, I. I. Mazin, and C. A. Howells, Phys. Rev. B **73**, 205102 (2006).
[18] P. B. Allen and R. C. Dynes, Phys. Rev. B **12**, 905 (1975).
[19] J. Wilson, F. Di Salvo, and S. Mahajan, Adv. Phys. **24**, 117 (1975).
[20] E. Morosan, H. W. Zandbergen, B. S. Dennis, J. W. G. Bos, Y. Onose, T. Klimczuk, A. P. Ramirez, N. P. Ong, and R. J. Cava, Nat. Phys. **2**, 544 (2006).
[21] D. Qian, D. Hsieh, L. Wray, E. Morosan, N. L. Wang, Y. Xia, R. J. Cava, and M. Z. Hasan, Phys. Rev. Lett. **98**, 117007 (2007).
[22] D. E. Moncton, J. D. Axe, and F. J. DiSalvo, Phys. Rev. Lett. **34**, 734 (1975).
[23] T. Yokoya, T. Kiss, A. Chainani, S. Shin, M. Nohara, and H. Takagi, Science **294**, 2518 (2001).
[24] M. D. Johannes and I. I. Mazin, Phys. Rev. B **77**, 165135 (2008).
[25] I. A. Nekrasov and M. V. Sadovskii, arXiv. 1205.5387 (2012).
[26] The Fermi surfaces, nesting functions, and the non-interacting electron response functions are calculated by fitting the LDA band structure using 64 maximally localized wannier orbitals and then interpolate the Hamiltonian on a $100 \times 100 \times 100$ Γ-centered K-mesh.